Aquatic Toxicology 150 (2014) 36–44

Contents lists available at ScienceDirect

Aquatic Toxicology

journal homepage: www.elsevier.com/locate/aquatox

Effects of chronic waterborne nickel exposure on growth, ion homeostasis, acid-base balance, and nickel uptake in the freshwater pulmonate snail, *Lymnaea stagnalis*

Som Niyogi [a,*], Kevin V. Brix [b], Martin Grosell [c]

[a] Department of Biology, University of Saskatchewan, Saskatoon, SK, Canada
[b] Department of Zoology, University of British Columbia, Vancouver, BC, Canada
[c] RSMAS, University of Miami, Miami, FL, USA

ARTICLE INFO

Article history:
Received 22 October 2013
Received in revised form 5 February 2014
Accepted 20 February 2014

Keywords:
Nickel
Snail
Chronic toxicity
Growth
Uptake kinetics
Ion homeostasis

ABSTRACT

The freshwater pulmonate snail, *Lymnaea stagnalis*, is the most sensitive aquatic organism tested to date for Ni. We undertook a series of experiments to investigate the underlying mechanism(s) for this observed hypersensitivity. Consistent with previous experiments, juvenile snail growth in a 21-day exposure was reduced by 48% relative to the control when exposed to 1.3 $\mu g\,l^{-1}$ Ni (EC_{20} less than the lowest concentration tested). Ca^{2+} homeostasis was significantly disrupted by Ni exposure as demonstrated by reductions in net Ca^{2+} uptake, and reductions in Ca^{2+} concentrations in the hemolymph and soft tissues. We also observed reduced soft tissue [Mg^{2+}]. Snails underwent a significant alkalosis with hemolymph pH increasing from 8.1 to 8.3 and hemolymph TCO_2 increasing from 19 to 22 mM in control versus Ni-exposed snails, respectively. Unlike in previous studies with Co and Pb, snail feeding rates were found to be unaffected by Ni at the end of the exposure. Snails accumulated Ni in the soft tissue in a concentration-dependent manner, and Ni uptake experiments with ^{63}Ni revealed a biphasic uptake profile – a saturable high affinity component at low exposure concentrations (36–189 nM) and a linear component at the high exposure concentrations (189–1897 nM). The high affinity transport system had an apparent K_m of 89 nM Ni^{2+} and V_{max} of 2.4 nmol g^{-1} h^{-1}. This equates to a log *K* of 7.1, significantly higher than log *K*'s (2.6–5.2) for any other aquatic organisms evaluated to date, which will have implications for Biotic Ligand Model development. Finally, pharmacological inhibitors that block Ca^{2+} uptake pathways in snails did not inhibit Ni uptake, suggesting that the uptake of Ni does not occur via Ca^{2+} uptake pathways. As with Cu and Pb, the exact mechanism for the significant disruption in Ca^{2+} homeostasis and reduction in juvenile snail growth remains unknown.

1. Introduction

Nickel (Ni) is an important contaminant present at elevated concentrations in many aquatic ecosystems that are currently, or have previously been, impacted by metal-mining activities (Eisler, 1998). Ni concentrations, which typically vary between 1 and 10 $\mu g\,l^{-1}$ in unimpacted freshwaters, may reach as high as several hundred to 1000 $\mu g\,l^{-1}$ in highly contaminated natural waters (Eisler, 1998). Although Ni is considered to be an essential micronutrient, its essentiality in aquatic animals is yet to be fully characterized (Muyssen et al., 2004). Ni is consistently found in the tissues of aquatic animals at low levels, even in the absence of elevated Ni exposure, and appears to be well regulated by most aquatic organisms (Chowdhury et al., 2008; Muyssen et al., 2004). Similar to the actions of other transition metals such as Cu and Zn, both deficiency and excess of Ni have been found to affect survival in algae and aquatic plants (Eisler, 1998; Muyssen et al., 2004).

Toxicity studies have indicated that the common freshwater pulmonate snail, *Lymnaea stagnalis*, is considerably more sensitive to chronic Ni exposure (EC_{20} for growth 4.4 $\mu g\,l^{-1}$) than other representative aquatic invertebrate species (Schlekat et al., 2010). Schlekat et al. (2010) suggested that *L. stagnalis* replaces the cladoceran, *Cerodaphnia dubia*, as the most sensitive aquatic species in the Ni ecotoxicity database adopted by European Union for regulatory risk assessment (European Chemicals Bureau, 2008). Recent field assessments have recorded similar Ni effect concentrations for snails in field bioassessment studies (Peters et al., 2014). These

* Corresponding author at: Department of Biology, University of Saskatchewan, 112 Science Place, Saskatoon SK S7N 5E2, Canada. Tel.: +1 306 966 4453.
E-mail address: som.niyogi@usask.ca (S. Niyogi).

http://dx.doi.org/10.1016/j.aquatox.2014.02.012
0166-445X/

observations are consistent with studies demonstrating that *L. stagnalis* is either the most sensitive or second most sensitive freshwater species in chronic exposures to Co, Cu and Pb (Brix et al., 2011; Schlekat et al., 2010; De Schamphelaere et al., 2008). Because of this high sensitivity to metals in chronic exposures, *L. stagnalis* has emerged as a model freshwater organism, and is particularly important in revisions to water quality criteria (WQC) for metals including WQC based on the biotic ligand model (BLM) (Peters et al., 2014; Schlekat et al., 2010).

The understanding of the physiological mechanisms that cause toxicity can provide a mechanistic foundation for the development of any BLM. It has been shown that juvenile snail growth is a sensitive endpoint for *L. stagnalis* during chronic exposure to Co, Cu and Pb, and that growth inhibition occurs concurrently with the disruption of Ca^{2+} uptake and homeostasis for these metals (Munley et al., 2013; Brix et al., 2011, 2012; Grosell and Brix, 2009; De Schamphelaere et al., 2008). Snails have a very high Ca^{2+} requirement for shell formation, particularly during early life stages, which was thought to be the basis of their high sensitivity to metals (Grosell and Brix, 2009). However, more recent studies have indicated that disruption of Ca^{2+} homeostasis in *L. stagnalis* might be a secondary effect of chronic metal exposures (Brix et al., 2011, 2012), and the primary mechanism(s) of toxicity remains elusive.

The physiological mechanism(s) of Ni toxicity in aquatic organisms is yet to be fully understood. In fish, Ni has been found to act primarily as a respiratory, rather than an ionoregulatory, toxicant in both acute and chronic exposures (Pane et al., 2003a,b, 2004a,b). In contrast, Ni appears to act more like an ionoregulatory toxicant in aquatic invertebrates, particularly in acute exposures. Pane et al. (2004a,b) suggested that Ni causes toxicity to *Daphnia* primarily via disruption of Mg^{2+}, and not Ca^{2+}, homeostasis in both acute and chronic exposures, although Pane and co-workers also recorded impaired respiratory functions during chronic exposure. Leonard and Wood (2013) reported that acute Ni exposure causes depletion of soft tissue Na^+ and Mg^{2+} levels in *L. stagnalis* at relatively high Ni exposure concentrations (~290 and 750 $\mu g\,l^{-1}$ Ni, respectively), providing further evidence of ionoregulatory toxicity by Ni. It remains to be examined though whether chronic Ni exposure causes disruption of ionoregulatory homeostasis in *L. stagnalis*. To this end, it is particularly interesting to investigate whether any potential ionoregulatory toxicity during Ni exposure is driven mainly by the disruption of Ca^{2+} homeostasis, as observed with other metals such as Pb, Co and Cu, or if Ni perturbs Mg^{2+}/Na^+ homeostasis as well.

The main objective of the present study was to enhance our understanding of the physiological mechanisms of chronic waterborne Ni toxicity to *L. stagnalis*. We conducted a chronic toxicity test with early life stages of *L. stagnalis*, in which we monitored growth (increase in body mass), feeding rate, Ni accumulation in soft tissues, hemolymph and soft tissue ion levels, acid-base balance, and net Ca^{2+} flux. In addition, using separate experiments we also examined the influence of Ni on unidirectional Na^+ influx rates, and the kinetic and pharmacological properties of short-term Ni uptake.

2. Materials and methods

2.1. Experimental animals

Adult snails were obtained from an in-house culture maintained in flow-through dechlorinated City of Miami tap water ($[Na^+] = 1.14$, $[Ca^{2+}] = 0.51$, $[Mg^{2+}] = 0.09$, $[Cl^-] = 1.03$, $[HCO_3^-] = 0.68\ mmol\,l^{-1}$, $[DOC] = 200\ \mu mol\,l^{-1}$, $pH = 7.8$) at 24–25 °C under a photoperiod of 16 h light:8 h dark (Brix et al., 2012). The culture was fed a mix of lettuce, carrots and sweet potatoes, and egg masses were transferred from the main culture tanks to static-renewal nursery tanks for hatching and juvenile growth before they were used in toxicity studies.

2.2. Chronic toxicity test

An early life stage chronic toxicity test (21–24 d) was performed beginning with juvenile (7–8 d old; 2–4 mg wet weight) snails. The experiment consisted of 5 Ni treatments (nominal concentrations: 1, 2, 4, 8 and 16 $\mu g\,l^{-1}$) and a control, with 10 replicates per treatment each consisting of an individual snail in a 250 ml polypropylene cup with 200 ml of test solution. Ni exposures were performed in dechlorinated City of Miami tap water under static renewal conditions at 25 ± 1 °C. A 100% water change was performed daily with test solutions that were made 24 h prior to use to allow for metal equilibration.

Snails were fed romaine lettuce daily at a rate sufficient to ensure food was continuously available, as this has been shown to be critical for ensuring maximum snail growth (Brix et al., 2012). Survival was monitored daily. Water samples were collected at the beginning of the experiment and daily thereafter for determination of dissolved Ni exposure concentrations. Samples were passed through a 0.45 μm cellulose nitrate syringe filter (Acro-disc, Pall Life Sciences, MI, USA), acidified by addition of HNO_3 (Trace metal grade, Fisher Scientific, USA) to a final concentration of 1%, and stored at 4 °C for analysis of dissolved Ni concentrations. On one occasion, water samples were also collected, immediately after the daily water exchange and 24 h later prior to the next water exchange, from 2 exposure cups selected randomly to assess any change in DOC level in the exposure water.

2.3. Characterization of growth and net Ca^{2+} flux rate

Snail growth (increase in body mass) and net Ca^{2+} flux rates in individual snails were determined on Days 7, 14, and 21. Snails were placed in individual containers that ranged from 1.5 ml centrifuge tubes to 100 ml polypropylene beakers (flux volume 0.9–80 ml) depending on the size of the snail. Snails were allowed to recover from handling for 10 min prior to flux initiation. Each container was gently aerated through polyethylene tubing and covered as appropriate for the container. At the onset of flux measurements, a water sample (0.1–2 ml depending on flux volume) was collected for measurement of Ca^{2+} concentration. After a total flux time of 2.5–7.5 h, (exact time for individual snails recorded) a second water sample was obtained from each beaker, after which the snails were removed from the flux beaker, rinsed, blotted dry and weighed to the nearest 0.01 mg on an analytical balance (Mettler Toledo, USA). The flux volume and duration for different sized snails were based on a previous study (Brix et al., 2012) to ensure that waterborne Ca^{2+} concentrations differed by at least ~50 μM Ca^{2+} over the flux period but did not drop below 200 μM (from an initial Ca^{2+} concentration of ~510 μM). A methods control experiment (without animals) demonstrated no loss of Ca^{2+} to test container walls during an 8 h flux period. Snails were not fed during the flux measurement. Net Ca^{2+} flux rates were determined as the change in total Ca^{2+} concentration from the beginning to the end of the flux period, accounting for the duration of the flux period and the mass of the snail (Grosell and Brix, 2009).

2.4. Characterization of feeding rate

Feeding rate in each snail was evaluated during day 22–23 of the exposure as described in Brix et al. (2012). Briefly, the relationship between lettuce wet weight (prior to being placed in test containers) and area was determined. Area of lettuce was determined by photographing the lettuce and digitally analyzing the

image using the free area analysis software Image J (available at http://rsb.info.nih.gov/ij). For the feeding rate experiment, individual pieces of lettuce were photographed and then placed with snails. Snails were allowed to feed on the lettuce for 24 h, after which the lettuce was removed and re-imaged. Differences in area before and after were then used to estimate the mass of lettuce consumed by individual snails and then normalized for differences in snail mass (weight of the food consumed per day (mg)/wet weight of snail (g)).

2.5. Sampling for acid-base balance and ion concentrations in hemolymph and soft tissues, and Ni accumulation on soft tissues

Acid-base balance and ion concentrations in extracellular fluids and soft tissue ion concentrations were determined in snails after 24 d of exposure to different Ni concentrations. A predatory avoidance reflex in *L. stagnalis* which expels substantial volumes of extracellular fluid in response to stimulation of the foot was utilized to obtain extracellular fluid samples. Extracellular fluid was collected in micro-centrifuge tubes by a pipette and a subsample was transferred to a separate 0.5 ml tube for immediate pH measurements. Following pH measurements, the subsamples were used to measure total CO_2 concentrations. The remaining extracellular fluid samples were stored at 4 °C for later analysis of Ca^{2+}, Mg^{2+} and Na^+.

Following sampling of extracellular fluids, snails were euthanized by freezing at −20 °C, thawed subsequently, and soft tissue was separated from the shell by dissection, weighed and digested in 1 N HNO_3 at 70 °C for 24 h prior to analysis of tissue Ca^{2+}, Mg^{2+} Na^+, and Ni.

2.6. Characterization of unidirectional Na^+ influx rate

Juvenile *L. stagnalis* (7–8 day old, 2–4 mg wet weight) were exposed to 0 (control) and 16 μg l^{-1} Ni in dechlorinated City of Miami tap water for 14 days under similar exposure conditions as described above for 21 d chronic bioassay. The only difference being that snails (10 per treatment) were maintained in 4 l polypropylene beakers containing 2 l exposure water. Following the exposure, unidirectional Na^+ flux rates were measured in individual snails as described in Grosell and Brix (2009). Briefly, 8 snails from each treatment were placed in individual polypropylene beakers each containing 15 ml of dechlorinated tap water and allowed to recover from handling for 10 min prior to the initiation of flux measurement. Each beaker was covered with Parafilm® and gently aerated through polyethylene tubing. At the onset of the Na^+ flux measurements, 0.02 μCi ^{22}Na (as NaCl; Amersham Biosciences, specific activity >100 mCi/mg Na^+) was added to each beaker and a 5 min equilibration period was allowed before water samples were obtained for ^{22}Na radioactivity and total Na^+ concentration analysis. After a total flux time of 2.5–3 h (exact time for individual snails recorded) a second water sample was obtained from each beaker after which the snails were removed from the flux beaker, rinsed, blotted dry and weighed. Unidirectional Na^+ uptake rates (nmol g^{-1} h^{-1}) were determined using the following equation:

$$J_{in}(\text{influx}) = \frac{(CPM\, g^{-1})/MSA}{t}$$

where CPM is the final radioactivity (counts min^{-1}) of ^{22}Na in the wholebody of snail, MSA is the mean specific activity of ^{22}Na in the water over the entire flux period and t is time.

2.7. Kinetic and pharmacological characterization of short-term Ni uptake

To evaluate the kinetic properties of short-term Ni uptake, juvenile snails (21 d old, ~150 mg wet weight) were exposed to 4, 8, 16, 40, 70, and 140 μg l^{-1} of radiolabeled Ni in dechlorinated Miami tap water for 7 h. Ni uptake was evaluated in individual snails (8 per treatment). The experimental set-up was similar to that used for unidirectional Na^+ influx measurement, except that a greater flux volume (28 ml) was used in this experiment. Exposure waters were first spiked with cold Ni and allowed to equilibrate for 24 h. At the onset of the Ni uptake measurements, 3.1 μCi ^{63}Ni (as $NiCl_2$; Amersham Biosciences) was added to each flux chamber. Water samples were collected at the beginning and end of the flux period from each flux chamber for ^{63}Ni radioactivity and total Ni concentration analysis. Ni uptake rates (nmol g^{-1} h^{-1}) were determined as described above for the measurement of unidirectional Na^+ influx rates.

To examine the pharmacological characteristics of Ni uptake, individual snails (8 per treatment) were exposed similarly to 16 μg l^{-1} of radiolabeled Ni, in the absence and presence of 4 different Ca^{2+} channel blockers. The Ca^{2+} channel blockers used in this experiment were lanthanum [10^{-4} M] (a voltage independent Ca^{2+} channel blocker (Kovács. et al., 1991)), nifedipine [10^{-5} M] (a dihydropyridine Ca^{2+} channel blocker (Buckley et al., 2007)), verapamil [10^{-4} and 10^{-5} M] (a L-type Ca^{2+} channel blocker (Buckley et al., 2007)) and EIPA [5×10^{-5} M] (a blocker of the Ca^{2+} permeable TRPP3 channel and possibly the $Ca^{2+}/2H^+$ exchanger (Dai et al., 2007)). Ni uptake rates (nmol g^{-1} h^{-1}) were evaluated following 5.5–6.5 h of Ni flux (exact time for individual snails recorded) as described above.

2.8. Analytical chemistry

Extracellular fluid pH was determined in 20–50 μl subsamples using an Accumet micro pH electrode coupled to a radiometer 220 pH meter (Radiometer, Copenhagen, Denmark). Concentrations of total CO_2 in hemolymph samples were analyzed using a Corning Carbon Dioxide Analyzer 965 (Essex, England).

Concentrations of ions (Ca^{2+}, Mg^{2+}, and Na^+) in the hemolymph, soft tissue digests, and exposure water samples (Ca^{2+} and Na^+ only) were determined by flame atomic absorption spectroscopy (VarianAA 220FS, Mulgrave, Victory, Australia), with a practical detection limit of 2 μM Ca^{2+} or Na^+, and 3 μM Mg^{2+}. Concentrations of Ni in the exposure water samples and soft tissue digests were analyzed by graphite furnace atomic absorption spectroscopy (Perkin Elmer AAnalyst 800, Shelton, Connecticut, USA), with a practical detection limit of 0.1 μg l^{-1} Ni. DOC concentration in the filtered exposure water was measured by high-temperature catalytic oxidation using a total organic carbon analyzer (Shimadzu TOC-VCSH, Kyoto, Japan), with a detection limit of 20 μmol l^{-1}.

Gamma radioactivity from ^{22}Na was analyzed using an automated gamma counter (Packard Cobra II Auto-Gamma, Meriden, Connecticut, USA). Beta radioactivity from ^{63}Ni was determined using an automated scintillation counter (TmAnalytical Beta Tract 6895, Austin, Texan, USA).

2.9. Data analysis

All analyses were performed on measured test concentrations. Data are presented as mean ± SEM. The effect of Ni (EC_{20}) on snail growth (increase in wet body mass over 21 day exposure) was estimated using the linear interpolation method (USEPA, 2002). To determine the kinetic characteristics of short-term Ni uptake in snails, the Ni influx rates were plotted against the estimated Ni^{2+} concentrations in the exposure water. Ni^{2+} concentrations were

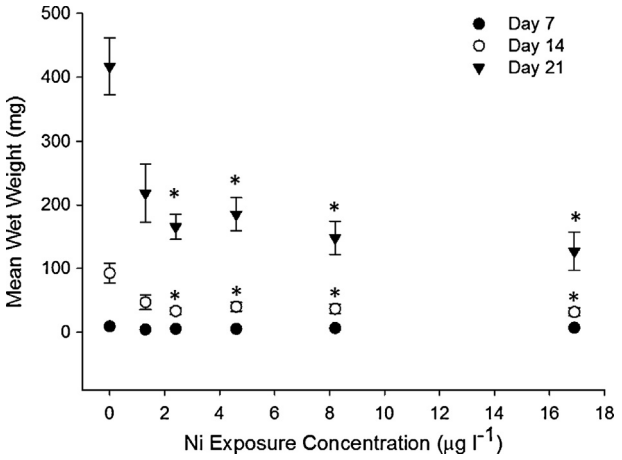

Fig. 1. Changes in body mass of juvenile *Lymnaea stagnalis* exposed to an increasing range of waterborne Ni over 21 days. Data are presented as mean ± SEM (n = 8–10). Asterisk indicates significant difference relative to the control (0 μg l^{-1} Ni) on the respective day of measurement.

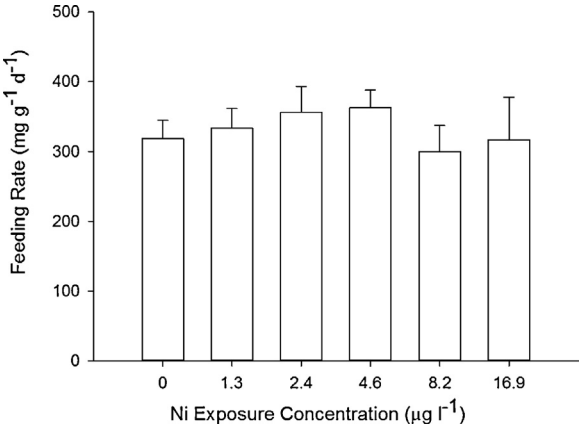

Fig. 2. Feeding rate of juvenile *Lymnaea stagnalis* exposed to an increasing range of waterborne Ni for 23 days. Data are presented as mean ± SEM (n = 8–10).

estimated by using Visual MINTEQ, version 3 (Gustafsson, 2010), which was supplied with the measured total dissolved Ni concentrations and the water chemistry data described above (major ions, pH and DOC). To model complexation of Ni^{2+} and DOC in Visual MINTEQ, we used NICA-Donnan option with humic acid and fulvic acid inputs of 50% each. Statistical evaluation of data from physiological studies was carried out using One Way ANOVA tests with a Dunnett post hoc test, except for unidirectional Na^+ flux data which was evaluated by Student's t-test. Results were considered statistically different at $p < 0.05$. Chronic toxicity data were analyzed using ToxCalc v5.0 (ToxCalc, 1996). All other analyses were performed using SigmaStat v11.0 (SPSS, 2006).

3. Results

3.1. Chronic Ni exposure and effects on survival, growth and feeding

Mean measured dissolved Ni concentrations were relatively close to the target nominal concentrations. The mean Ni concentration in the control exposure (dilution water) was below the detection limit (0.1 μg l^{-1}), and therefore presented as 0 μg l^{-1}. The mean Ni concentrations in the treatments were 1.3 ± 0.1, 2.4 ± 0.1, 4.6 ± 0.3, 8.2 ± 0.3, 16.9 ± 0.2 (n = 25 for each), respectively. The initial and final average DOC concentrations in the exposure water were 190 and 192 μmol l^{-1}, respectively.

No snail mortality was observed during over the 21 day chronic exposure except one death each in the 1.3 and 16.9 μg l^{-1} Ni exposure treatments. Individual snail weight was measured on Days 7, 14, and 21. No concentration-response on growth was observed over the first 7 days of exposure, as no significant difference was recorded in body mass among the six treatments (Fig. 1). However, a pronounced dose-dependent effect on growth was observed on both day 14 and 21, with a significant decrease in body mass occurring at Ni exposure concentrations of ≥2.4 μg l^{-1} relative to the control (Fig. 1). Over the 21 days of exposure, the increase in body mass at the highest Ni exposure concentration tested (16.9 μg l^{-1}) was approximately a third relative to that in the control (Fig. 1). Analysis of day 21 snail growth data (based on wet weight) resulted in an estimated EC_{20} below the lowest concentration tested and so is reported as <1.3 μg l^{-1} Ni. The lettuce consumption rate in snails was evaluated during day 22–23 of the exposure, and the percentage consumption of lettuce varied between 12 and 15 across the six treatments. No significant effect was observed in any Ni exposure treatments relative to the control (Fig. 2).

3.2. Effects of chronic Ni exposure on ion flux

Net Ca^{2+} flux was measured in snails on Day 7, 14 and 21. Net Ca^{2+} flux rate was generally lower during the first 7 days, reaching its maximum during the middle of the exposure followed by a minor decrease at the end, in more or less all treatment groups (Fig. 3). No effect of waterborne Ni exposure was recorded on Day 7 (Fig. 3A). However, there was a decreasing trend of net Ca^{2+} flux at exposure concentrations of ≥4.6 μg l^{-1} Ni on both Day 14 and 21, although a statistically significant was observed only at the highest exposure concentration (16.9 μg l^{-1}) examined (Fig. 3B and C). The effect of waterborne Ni exposure on net Ca^{2+} flux was most pronounced on day 14, with a 55% decrease at the highest exposure level relative to the control.

The effect of waterborne Ni on Na^+ influx was measured in snails exposed only to the highest exposure level [measured: 16.3 ± 0.6 Ni (n = 14)] for 14 days, and no significant difference was recorded relative to the control (Fig. 4).

3.3. Effects of chronic Ni exposure on ion concentrations and acid-base balance in hemolymph and soft tissue

There was a concentration dependent effect of waterborne Ni exposure on hemolymph Ca^{2+} concentration of snails, with a significant decrease occurring at ≥2.4 μg l^{-1} (Fig. 5). A 54% reduction of hemolymph Ca^{2+} was recorded at the highest exposure level relative to the control. There was, however, no effect of waterborne Ni exposure on hemolymph Na^+ and Mg^{2+} concentration (see Supplementary Table 1). Hemolymph pH increased gradually with increasing Ni exposure level, although significant differences relative to the control were only observed at 8.2 and 16.9 μg l^{-1} Ni (Fig. 6A). Hemolymph TCO_2 level also increased at Ni exposure concentrations of ≥2.4 μg l^{-1} (except at 8.2 μg l^{-1}) (Fig. 6B).

Supplementary material related to this article can be found, in the online version, at http://dx.doi.org/10.1016/j.aquatox.2014.02.012.

Both Ca^{2+} and Mg^{2+} levels in soft tissues were affected at the end of the chronic waterborne Ni exposure, with significant reductions relative to the control recorded at the highest Ni exposure concentration examined (16.9 μg l^{-1}) (Fig. 7A and B). However, chronic waterborne Ni exposure did not influence the Na^+ levels in soft tissues of snails (see Supplementary Table 1).

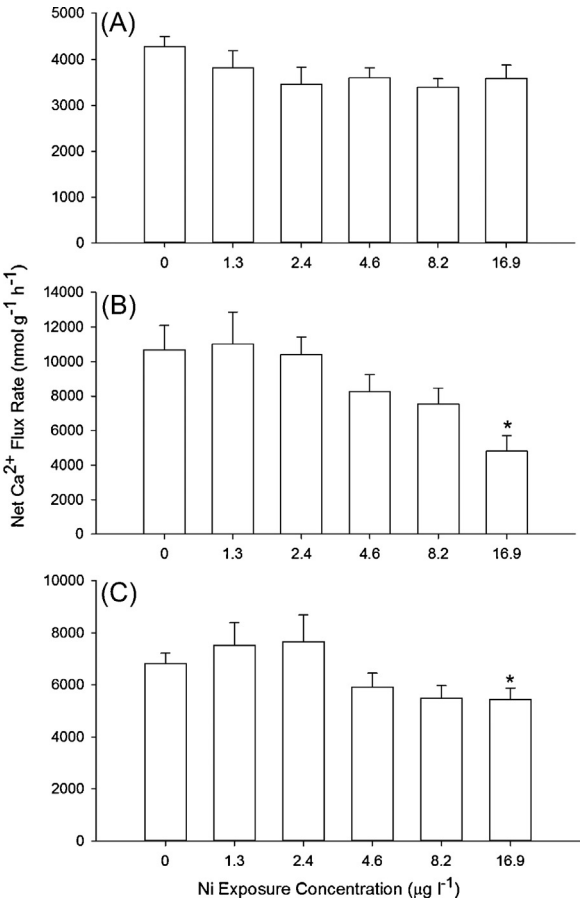

Fig. 3. Effects of 21 day waterborne Ni exposure on net Ca^{2+} flux in juvenile *Lymnaea stagnalis*, at day 7 (A), day 14 (B) and day 21 (C). Data are presented as mean ± SEM (n = 8–10). Asterisk indicates significant difference relative to the control (0 μg l^{-1} Ni).

3.4. Ni bioaccumulation, and kinetic and pharmacological properties

Ni accumulation in the soft tissues of snails showed an increasing trend with increasing waterborne Ni exposure, although a significant increase relative to the control was observed only at the two highest exposure concentrations tested (8.2 and 16.9 μg l^{-1}) (Fig. 8). Ni accumulation in snails increased by 4.5-fold at 16.9 μg l^{-1} Ni exposure relative to the control.

The average measured dissolved Ni exposure concentrations employed for examining the kinetics of short-term Ni uptake in snails were 3.3 ± 0.6, 8.2 ± 0.8, 15.5 ± 0.7, 36.7 ± 1.1, 65.8 ± 1.0, and 136.5 ± 1.2 μg l^{-1} (n = 16 for each). This corresponded to Ni^{2+}

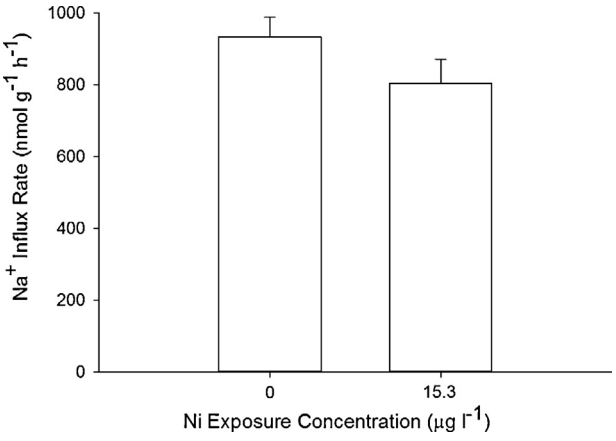

Fig. 4. Unidirectional Na^+ influx in juvenile *Lymnaea stagnalis* exposed to control (0 μg l^{-1} Ni) and elevated waterborne Ni (15.3 μg l^{-1} Ni) for 14 days. Data are presented as mean ± SEM (n = 8).

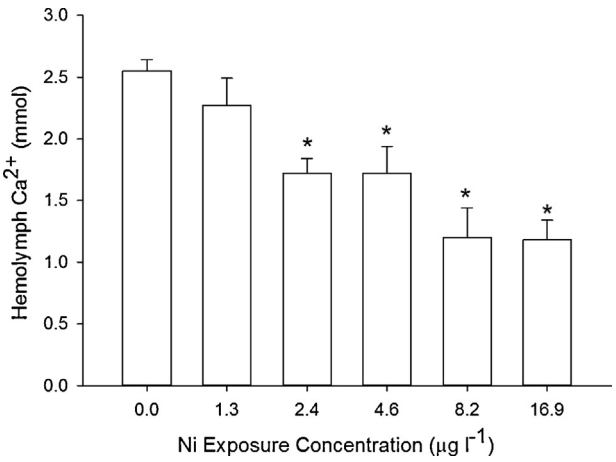

Fig. 5. Concentration of hemolymph Ca^{2+} in juvenile *Lymnaea stagnalis* exposed to an increasing range of waterborne Ni for 24 days. Data are presented as mean ± SEM (n = 8–10). Asterisk indicates significant difference relative to the control (0 μg l^{-1} Ni).

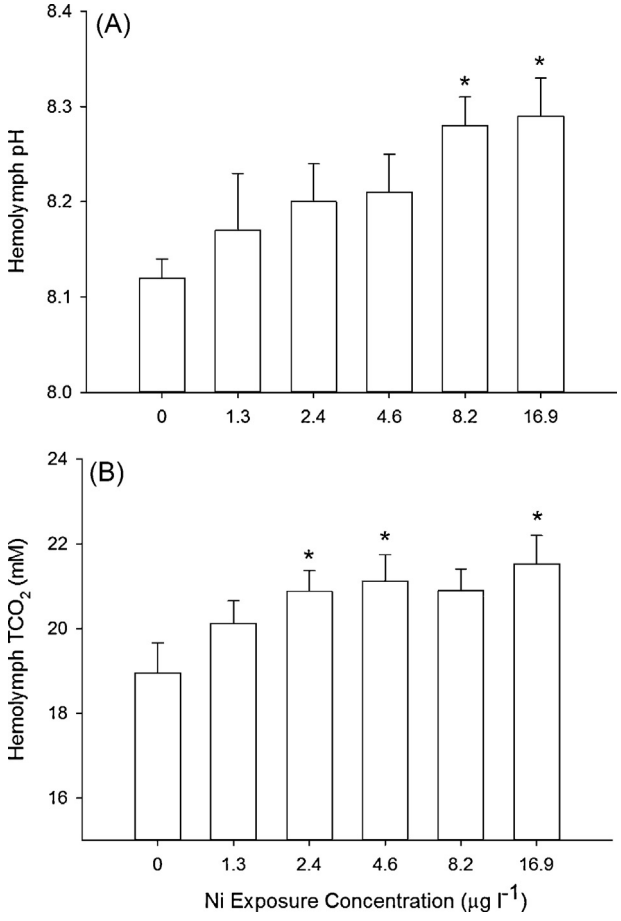

Fig. 6. Changes in hemolymph pH (A) and TCO_2 level (B) in juvenile *Lymnaea stagnalis* exposed to an increasing range of waterborne Ni for 24 days. Data are presented as mean ± SEM (n = 8–10). Asterisk indicates significant difference relative to the control (0 μg l^{-1} Ni).

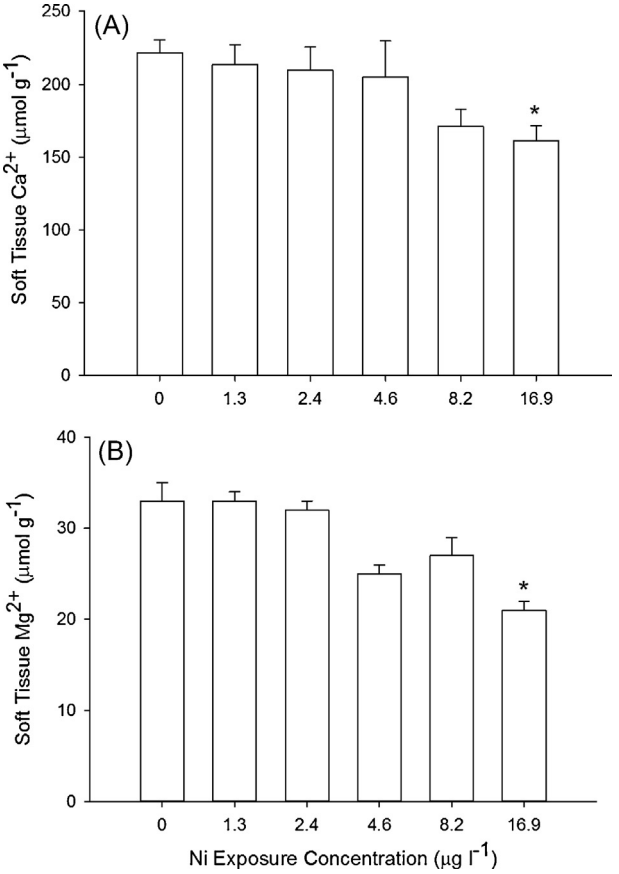

Fig. 7. Concentration of Ca^{2+} (A) and Mg^{2+} (B) in the soft tissues of juvenile *Lymnaea stagnalis* exposed to an increasing range of waterborne Ni for 24 days. Data are presented as mean ± SEM (n = 8–10). Asterisk indicates significant difference relative to the control (0 µg l^{-1} Ni).

exposure concentration of 36, 96, 189, 485, 892 and 1897 nM, respectively [as estimated by Visual MINTEQ, version 3 (Gustafsson, 2010)]. A bi-phasic profile of Ni uptake was observed, with an apparently saturable uptake recorded at the lower exposure concentrations (36–189 nM), followed by a linear uptake at the higher

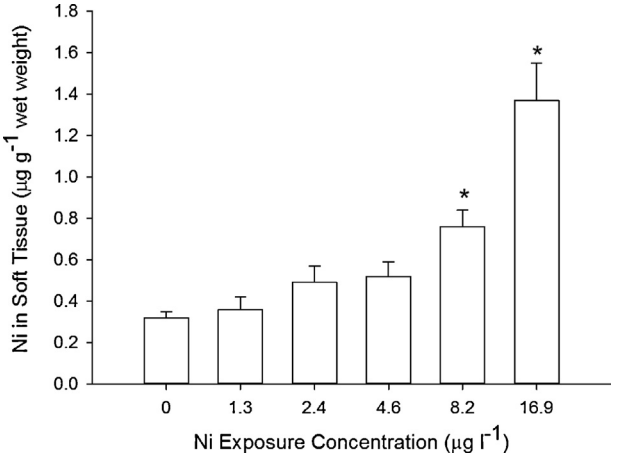

Fig. 8. Ni accumulation in the soft tissues of juvenile *Lymnaea stagnalis* exposed to an increasing range of waterborne Ni for 24 days. Data are presented as mean ± SEM (n = 8–10). Asterisk indicates significant difference relative to the control (0 µg l^{-1} Ni).

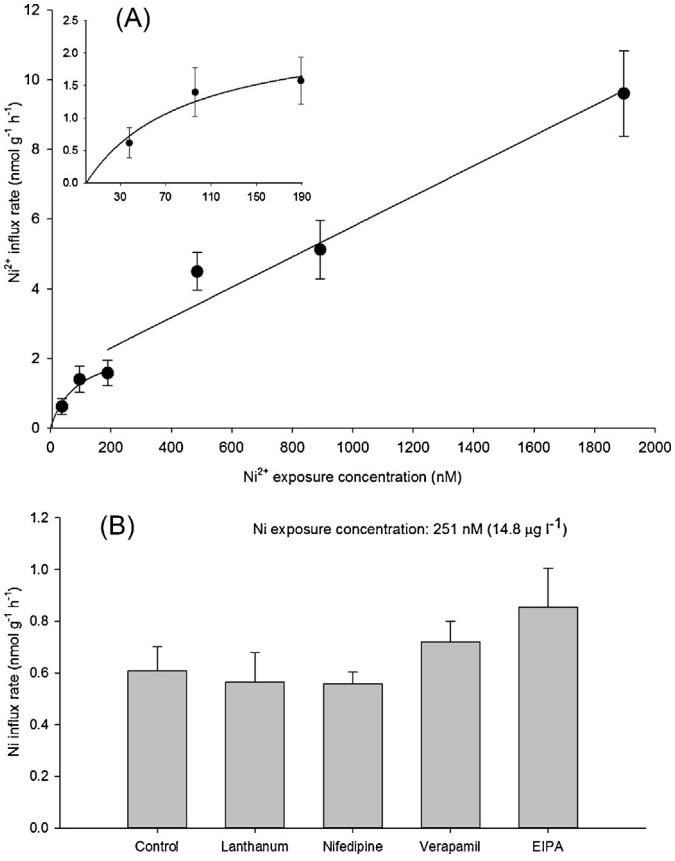

Fig. 9. (A) Concentration-dependent short-term waterborne Ni uptake in juvenile *Lymnaea stagnalis*. The uptake data for Ni^{2+} exposure range 36–189 nM were fitted with the Michaelis–Menten equation (presented separately in the inset Fig.), whereas a linear regression was used to fit the uptake data for Ni exposure range 189–1897 nM. Ni^{2+} concentration in the exposure water was estimated using Visual MINTEQ, version3 (Gustafsson, 2010). (B) Effects of different Ca^{2+} blockers on short-term Ni uptake in juvenile *Lymnaea stagnalis* exposed to 14.8 µg l^{-1} (251 nM) of waterborne Ni. Data are presented as mean ± SEM (n = 8).

exposure levels (189–1897 nM) (Fig. 9A). The kinetics of saturable Ni uptake was analyzed using the Michaelis–Menten equation:

$$J_{in} = \frac{J_{max} \times [X]}{[X] + K_m}$$

where J_{in} is the Ni uptake rate, [X] is the Ni^{2+} concentration in the exposure water, J_{max} is the maximum uptake rate, and K_m is the concentration of dissolved Ni^{2+} that resulted in half-maximal uptake rate (an index of uptake affinity). The apparent J_{max} and K_m of Ni uptake at the lower Ni exposure range, which corresponded with the Ni exposure range employed in the chronic toxicity test, was calculated to be 2.4 nmol g^{-1} h^{-1} and 89 nM, respectively.

The effects of different Ca^{2+} channel blockers on short-term waterborne Ni uptake were examined at an exposure concentration of 14.8 ± 0.6 µg l^{-1} (i.e., 251 nM) Ni (n = 80). None of the Ca^{2+} channel blockers tested had any influence on waterborne Ni uptake by snails (Fig. 9B).

4. Discussion

4.1. Relative sensitivity of L. stagnalis to Ni

As has been observed for other metals (e.g., Co, Cu, Pb), growth was a much more sensitive endpoint than survival for *L. stagnalis* chronically exposed to Ni. We observed *L. stagnalis* to be extremely sensitive to chronic Ni exposure with an EC_{20} (growth)

of <1.3 μg l^{-1}, the lowest concentration tested. This result is comparable to that observed by Schlekat et al. (2010), who reported an EC10 of <2 μg l^{-1} in water with a similar composition. As discussed in the analysis by Schlekat et al. (2010), these data indicate that *L. stagnalis* is the most sensitive aquatic organism tested to date for Ni. Hence, developing a detailed understanding of the mechanisms underlying this hypersensitivity is important in the development of BLM-based water quality guidelines/criteria.

4.2. Effects of Ni exposure on ion homeostasis and acid-base balance

Similar to other metals studied (Cu, Pb), we observed a significant inhibition of net Ca^{2+} uptake in snails exposed to Ni. As with previous studies on Pb (Brix et al., 2012), this inhibition was not immediate (no effects on Day 7), but by Day 14, a concentration response for net Ca^{2+} uptake was observed. There was some indication of recovery on Day 21, but significant effects were still observed at 16.9 μg l^{-1} Ni. Additionally, when snails were terminally sampled on Day 24, we observed a significant reduction in hemolymph Ca^{2+} at ≥2.4 μg l^{-1} Ni and soft tissue Ca^{2+} at 16.9 μg l^{-1} Ni, indicating there was still a profound disturbance of Ca^{2+} homeostasis at the end of the experimental exposure. The significant reduction in hemolymph Ca^{2+} contrasts with experiments on Pb, where hemolymph Ca^{2+} was maintained in snails despite significant reductions in net Ca^{2+} uptake and soft tissue Ca^{2+} concentrations (Grosell and Brix, 2009). Hence, while both metals (and Cu) are potent disruptors of Ca^{2+} homeostasis in *L. stagnalis*, there appear to be some differences in the exact mechanisms of this effect.

We had previously postulated based on detailed time course experiments, that while Pb clearly disrupt Ca^{2+} homeostasis in *L. stagnalis*, the mechanism of action was not direct inhibition of Ca^{2+} uptake pathways (e.g., Ca^{2+} channels, $Ca^{2+}/2H^{+}$ exchanger, Ca^{2+}-ATPase). As just mentioned, Ni appears to follow a similar delayed time course. Further support for indirect inhibition of Ca^{2+} uptake was provided by Leonard and Wood (2013) who observed no reduction in soft tissue Ca^{2+} concentrations after a 96 h exposure to very high Ni concentrations (up to 458 μg l^{-1}). The availability of a suitable radio-isotope for Ni allowed us to test this hypothesis more directly using a series of pharmacological inhibitors that target Ca^{2+} transport proteins in the apical membrane. These inhibitors have been previously shown to inhibit Ca^{2+} uptake in *L. stagnalis* (Ebanks et al., 2010a). However, none of the inhibitors was effective in reducing Ni uptake, providing evidence that Ni is not being taken up at or directly inhibiting Ca^{2+} uptake pathways in a competitive manner (Fig. 9B). However, non-competitive inhibition by Ni of components of the Ca^{2+} uptake pathways cannot be dismissed.

In addition to disruption of Ca^{2+} homeostasis, we also observed a significant reduction in soft tissue Mg^{2+} concentrations with a flat concentration response over the range of 4.6–16 μg l^{-1} Ni (Fig. 7B). Leonard and Wood (2013) observed a similar reduction in soft tissue Mg^{2+} after just 96 h with the same flat dose response over a much wider range of Ni concentrations (5.8–458 μg l^{-1}). The finding that Ni disrupts Mg^{2+} homeostasis is not novel. Previous studies have shown Ni disrupts Mg^{2+} uptake and whole body Mg^{2+} concentrations in *Daphnia magna* (Pane et al., 2003a,b) and Mg^{2+} re-absorption in the kidney of rainbow trout (Pane et al., 2005). The vertebrate Mg^{2+} transporter SLC41a1 is primarily responsible for Mg^{2+} transport in the fish kidney (Islam et al., 2013) but the prokaryotic homologue of SLC41 (MgtE) is not inhibited by Ni (Sahni and Scharenberg, 2013; Smith et al., 1995). There are several Mg^{2+} transporters (CorA, MgtA, MgtB) in prokaryotes that are inhibited by Ni (Snavely et al., 1991). However, the eukaryotic homologues of CorA (Mrsp2p and MRS2) are restricted to the inner mitochondrial membrane, while MgtA and MgtB have no apparent eukaryotic homologues (Kehres and Maguire, 2002). Given the above, it is unclear whether Ni is directly inhibiting Mg^{2+} transport in snails or whether observed disruption of Mg^{2+} homeostasis is the result of indirect effects similar to Ca^{2+}. In order to clarify this, future studies should focus on examining the effects of pharmacological agents, which are known to inhibit Mg^{2+} transport, on waterborne Ni uptake in snails.

Finally we also observed a marked alkalosis in Ni-exposed snails, with hemolymph total CO_2 and pH increasing in a concentration-responsive manner with significant effects at ≥2.4 and ≥8.2 μg l^{-1} Ni, respectively (Fig. 6). This is similar to effects previously observed in snails exposed to Pb (Grosell and Brix, 2009), but contrasts with the acidosis observed in snails exposed to Cu (Brix et al., 2011). As previously hypothesized for Pb-exposed snails (Grosell and Brix, 2009), we suggest the alkalosis in Ni-exposed snails was an indirect effect caused by continued production of HCO_3^- (via carbonic anhydrase mediated hydration of H_2O) in snail mantle despite reduced Ca^{2+} available for the consumption of this HCO_3^- for shell formation.

4.3. Chronic Ni accumulation in tissues, and kinetics of short-term Ni uptake

Ni accumulated in the soft tissues of snails in a concentration-dependent manner after 24 days of exposure with no evidence of Ni regulation (Fig. 8). The experiment measuring Ni uptake rates appeared to characterize 2 separate transport systems with a high affinity system displaying Michaelis–Menten type saturation kinetics while uptake in the low affinity system appeared linear as a function of exposure concentration (Fig. 9A). The high affinity system, which is most relevant for chronic toxicity, had an estimated K_m of 89 nM dissolved Ni^{2+}, which equates to a log K (an indicator of Ni^{2+} binding affinity) of 7.1.

The log K for Ni^{2+} estimated in the current study is substantially higher than the log K of 5.2 estimated by Leonard and Wood (2013) for acute (96 h) toxicity to *L. stagnalis* in water with a similar ionic composition or any other log K estimated for acute Ni toxicity or bioaccumulation (log K = 2.6–5.2) on other invertebrates and fish (Niyogi and Wood, 2004; Kozlova et al., 2009; Leonard and Wood, 2013). There are several possible factors contributing to the distinctly higher log K estimated in this study. First, the log K in this study is based on bioaccumulation data while many of the other log K's are based on toxicity data, although Leonard and Wood (2013) generally found good agreement between log K's derived using the two data types. Second, the log K in this study is based on only the high affinity transport system, while the log K's in Leonard and Wood (2013) consider a much wider range of exposure concentrations (which is appropriate for acute toxicity) and were not designed to distinguish between high and low affinity transport systems.

It is important to note that the high affinity transport system encompasses the range over which chronic toxicity occurs in *L. stagnalis* and so is likely appropriate for parameterizing a chronic Ni BLM for this species. This highlights the critical importance of properly characterizing BLM parameters for a new test organism or endpoint (e.g., acute vs. chronic). Several recent studies in which existing BLMs have been applied to new species or endpoints have focused on adjusting the LA_{50} or intrinsic sensitivity (Q_s) (De Schamphelaere et al., 2005; De Schamphelaere and Janssen, 2010; Meyer and Adams, 2010; Schlekat et al., 2010). While the LA_{50} or Q_s is likely to change for new species or acute vs. chronic toxicity, our data in conjunction with data from Leonard and Wood (2013), clearly shows that this is not the only parameter that will vary and attributing all of the differences between different species or acute

vs. chronic toxicity to the LA_{50} or Q_s will likely lead to mechanistically flawed BLMs.

4.4. Physiological mechanisms of Ni toxicity

It is unclear at this time what the exact underlying mechanism(s) of Ni toxicity is for *L. stagnalis*. Similar to studies on Co, Cu, and Pb, we demonstrated a significant disruption of both Ca^{2+} homeostasis and acid-base balance, with an additional disruption of Mg^{2+} homeostasis observed for Ni. Given that the various pharmacological inhibitors targeting Ca^{2+} uptake pathways did not affect Ni uptake (Fig. 9B), it is unlikely that Ni is directly inhibiting Ca^{2+} uptake in a competitive manner, again similar to results for Cu and Pb. In contrast to studies on Co and Pb (De Schamphelaere et al., 2008; Brix et al., 2012), feeding rate was not inhibited in Ni-exposed snails, indicating that while there are many similarities in mechanisms of action between these metals, there are also significant differences. Although it is to be noted here that in the present study the feeding rate in snails was estimated at the end of 21 day Ni exposures, and thus it is possible that feeding might have been affected during the early phases of exposure but recovered by day 21.

Finally, we note that *L. stagnalis* is very sensitive to Co (De Schamphelaere et al., 2008), Cu (Brix et al., 2011), Pb (Brix et al., 2012), and Ni (Schlekat et al., 2010), but relatively insensitive to Zn (De Schamphelaere and Janssen, 2010), a well-documented Ca^{2+}-antagonist (Wood, 2001). Interestingly, *L. stagnalis* poorly regulates the body burdens (i.e., high accumulation) of metals (Co, Cu, Ni, Pb) to which it is sensitive (Pyatt et al., 1997; Amiard and Amiard-Triquet, 1979; Pyatt et al., 2003; Croteau and Luoma, 2009), but does regulate Zn (Desouky et al., 2003). This inability to regulate body burdens and presumably accumulation at whatever target tissues are eliciting hypersensitivity to metals may suggest a common mechanism of action for Co, Cu, Ni, and Pb, but not Zn. A more detailed comparative study of metal homeostasis for both toxic and relatively non-toxic metals to *L. stagnalis* might provide further insight into the mechanisms of toxic action for both groups of metals.

5. Conclusions

Overall, the present study demonstrated that the growth of freshwater pulmonate snail *L. stagnalis* is affected by very low level of chronic Ni exposure. We also found that Ni exposure reduces net Ca^{2+} uptake, disrupts Ca^{2+} and Mg^{2+} homeostasis, and induces alkalosis in these animals. The feeding rate estimated at the end of the 21 day chronic Ni exposures was found to be unaffected by chronic Ni exposure – indicating that growth reduction might not have resulted from the lack of nutrition. *L. stagnalis* seems to accumulate waterborne Ni in soft tissues in a concentration dependent manner, and the affinity of short-term Ni uptake ($\log K$) at the low exposure concentrations in this species appears to be much higher relative to that in any other freshwater species previously examined. Interestingly, although net Ca^{2+} uptake was strongly influenced by Ni exposure, pharmacological examination revealed that Ni uptake does not occur via Ca^{2+} uptake pathways. Further research is required to identify the mechanism(s) of interactions between Ca^{2+} and Ni, and to understand why *L. stagnalis* is extremely sensitive to chronic Ni exposure.

Acknowledgements

SN is supported by research funds from NSERC (Discovery Grant: 312017-2011) and University of Saskatchewan. KVB was supported by an NSF Graduate Research Fellowship, NSF Post-Doctoral Fellowship, and the SETAC/ICA Chris Lee Award for Metals Research.

References

Amiard, J.C., Amiard-Triquet, C., 1979. Distribution of cobalt 60 in a mollusc, a crustacean and a freshwater teleost: variation as a function of the source of pollution and during elimination. Environ. Pollut. 20, 199–213.
Brix, K.V., Esbaugh, A.J., Grosell, M., 2011. The toxicity and physiological effects of copper on the freshwater pulmonate snail, *Lymnaea stagnalis*. Comp. Biochem. Physiol. 154C, 261–267.
Brix, K.V., Esbaugh, A.J., Munley, K.M., Grosell, M., 2012. Investigations into the mechanism of lead toxicity to the freshwater pulmonate snail, *Lymnaea stagnalis*. Aquat. Toxicol. 106-107, 147–156.
Buckley, N., Dawson, A., Whyte, I., 2007. Calcium channel blockers. Medicine 35, 599–602.
Chowdhury, M.J., Bucking, C., Wood, C.M., 2008. Is nickel an essential metal for aquatic animals. Integr. Environ. Assess. Manag. 4, 266–268.
Croteau, M.N., Luoma, S.N., 2009. Predicting dietborne metal toxicity from metal influxes. Environ. Sci. Technol. 43, 4915–4921.
Dai, X-Q., Ramji, A., Liu, Y., Li, Q., Karpinski, E., Chen, X-Z., 2007. Inhibition of TRPP3 channel by amiloride and analogs. Mol. Pharmacol. 72, 1576–1585.
De Schamphelaere, K.A.C., Janssen, C.R., 2010. Cross-phylum extrapolation of the *Daphnia magna* chronic biotic ligand model for zinc to the snail *Lymnaea stagnalis* and the rotifer *Brachionus calyciflorus*. Sci. Total Environ. 408, 5414–5422.
De Schamphelaere, K.A.C., Koene, J.M., Heijerick, D.G., Janssen, C.R., 2008. Reduction of growth and haemolymph Ca levels in the freshwater snail *Lymnaea stagnalis* chronically exposed to cobalt. Ecotoxicol. Environ. Saf. 71, 65–70.
De Schamphelaere, K.A.C., Lofts, S., Janssen, C.R., 2005. Bioavailability models for predicting acute and chronic toxicity of zinc to algae, daphnids, and fish in natural surface waters. Environ. Toxicol. Chem. 24, 1190–1197.
Desouky, M.M., McCrohan, C.R., Jugdaohsingh, R., Powell, J.J., White, K.N., 2003. Effect of orthosilicic acid on the accumulation of trace metals by the pond snail *Lymnaea stagnalis*. Aquat. Toxicol. 64, 63–71.
Ebanks, S.C., O'Donnell, M.J., Grosell, M., 2010. Characterization of mechanisms for Ca^{2+} and HCO_3^-/CO_3^{2-} acquisition for shell formation in embryos of the freshwater common pond snail *Lymnaea stagnalis*. J. Exp. Biol. 213, 4092–4098.
Eisler, R., 1998. Nickel Hazards to Fish, Wildlife, and Invertebrates: A Synoptic Review. U.S. Department of the Interior, Washington, D.C., pp. 76.
European Chemicals Bureau, 2008. European Risk Assessment Report: Nickel, Ispra, Italy.
Grosell, M., Brix, K.V., 2009. High net calcium uptake explains the hypersensitivity of the freshwater pulmonate snail, *Lymnaea stagnalis*, to chronic lead exposure. Aquat. Toxicol. 91, 302–311.
Gustafsson, J.P., 2010. Visual MINTEQ. Land Water Res. Eng., Stoholm, Sweden.
Islam, Z., Hayashi, N., Yamamoto, Y., Doi, H., Romero, M.F., Hirose, S., Kato, A., 2013. Identification and proximal tubular localization of the Mg2+ transporter, Slc41a1, in a seawater fish. Am. J. Physiol. 305, R385–R396.
Kehres, D.G., Maguire, M.E., 2002. Structure, properties and regulation of magnesium transport proteins. BioMetals 15, 261–270.
Kovács., T., Csákány, B., Török, A., Csillik, B., 1991. Effects of lanthanum-induced blockade of calcium channels on nerve regeneration. Journal fur Hirnforschung 32, 195–201.
Kozlova, T., Wood, C.M., McGeer, J.C., 2009. The effect of water chemistry on the acute toxicity of nickel to the cladoceran *Daphnia pulex* and the development of a biotic ligand model. Aquat. Toxicol. 91, 221–228.
Leonard, E.N., Wood, C.M., 2013. Acute toxicity, critical body residues, Michaelis–Menten analysis of bioaccumulation, and ionoregulatory disturbance in response to waterborne nickel in four invertebrates: *Chironomus riparius*, *Lymnaea stagnalis*, *Lumbriculus variegatus*, and *Daphnia pulex*. Comp. Biochem. Physiol. 158C, 10–21.
Meyer, J.S., Adams, W.J., 2010. Relationship between biotic ligand model-based water quality criteria and avoidance and olfactory responses to copper by fish. Environ. Toxicol. Chem. 29, 2096–2103.
Munley, K.M., Brix, K.V., Panlilio, J., Grosell, M., 2013. Growth inhibition in early life-stage tests predicts full life-cycle toxicity effects of lead on the freshwater pulmonate snail, *Lymnaea stagnalis*. Aquat. Toxicol. 128–129, 60–66.
Muyssen, B.T.A., Brix, K.V., DeForest, D.K., Janssen, C.R., 2004. Nickel essentiality and homeostasis in aquatic organisms. Environ. Rev. 12, 113–131.
Niyogi, S., Wood, C.M., 2004. Biotic ligand model, a flexible tool for developing site-specific water quality guidelines for metals. Environ. Sci. Technol. 38, 6177–6192.
Pane, E.F., Bucking, C., Patel, M., Wood, C.M., 2005. Renal function in the freshwater rainbow trout (*Oncorhynchus mykiss*) following acute and prolonged exposure to waterborne Ni. Aquat. Toxicol. 72, 119–133.
Pane, E.F., Haque, A., Wood, C.M., 2004a. Mechanistic analysis of acute, Ni-induced respiratory toxicity in the rainbow trout (*Oncorhynchus mykiss*): an exclusively branchial phenomenon. Aquat. Toxicol. 69, 11–24.
Pane, E.F., McGeer, J.C., Wood, C.M., 2004b. Effects of chronic waterborne nickel exposure on two successive generations of *Daphnia magna*. Environ. Toxicol. Chem. 23, 1051–1056.
Pane, E.F., Richards, J.G., Wood, C.M., 2003a. Acute waterborne nickel toxicity in the rainbow trout (*Oncorhynchus mykiss*) occurs by a respiratory rather than ionoregulatory mechanism. Aquat. Toxicol. 63, 65–82.

Pane, E.F., Smith, C., McGeer, J.C., Wood, C.M., 2003b. Mechanisms of acute and chronic waterborne nickel toxicity in the freshwater cladoceran, *Daphnia magna*. Environ. Sci. Technol. 37, 4382–4389.

Peters, A., Simpson, P., Merrington, G., Schlekat, C.E., Rogevich-Garman, E., 2014. Assessment of the effects of nickel on benthic macro invertebrates in the field. Environ. Sci. Pollut. Res. 21, 193–204.

Pyatt, F.B., Metcalfe, M.R., Pyatt, A.J., 2003. Copper bioaccumulation by the freshwater snail *Lymnaea peregra*: a toxicological marker of environmental and human health? Environ. Toxicol. Chem. 22, 561–564.

Pyatt, F.B., Pyatt, A.J., Pentreath, V.W., 1997. Distribution of metals and accumulation of lead by different tissues in the freshwater snail *Lymnaea stagnalis* (L.). Environ. Toxicol. Chem. 16, 1393–1395.

Sahni, J., Scharenberg, A.M., 2013. The SLC41 family of MgtE-like magnesium transporters. Mol. Aspects Med. 34, 620–628.

Schlekat, C.E., Van Genderen, E.J., De Schamphelaere, K.A.C., Antunes, P.M.C., Rogevich, E.C., Stubblefield, W.A., 2010. Cross-species extrapolation of chronic nickel Biotic Ligand Models. Sci. Total Environ. 408, 6148–6157.

Smith, R.L., Thompson, L.J., Maguire, M.E., 1995. Cloning and characterization of MgtE, a putative new class of Mg^{2+} transporter from *Bacillus firmus* OF4. J. Bacteriol. 177, 1233–1238.

Snavely, M.D., Gravina, S.A., Cheung, T.T., Miller, C.G., Maguire, M.E., 1991. Magnesium transport in *Salmonella typhimurium*: regulation of *mgtA* and *mgtB* expression. J. Biol. Chem. 266, 824–829.

SPSS, 2006. SigmaStat 3.5. SPSS, Chicago, IL.

ToxCalc, 1996. ToxCalc. Tidepool Scientific Software, McKinleyville, California.

USEPA, 2002. Short-term Methods for Estimating the Chronic Toxicity of Effluents and Receiving Waters to Freshwater Organisms. U.S. Environmental Protection Agency, Cincinatti, OH, 350 pp.

Wood, C.M., 2001. Toxic responses of the gill. In: Schlenk, D.W., Benson, W.H. (Eds.), Target Organ Toxicity in Marine and Freshwater Teleosts, volume 1 – Organs. Taylor and Francis, Washington DC, pp. 1–89.